5-Ethynyluridine

Maassen, Sjors; Coenen, Britt; Dulk, Sara; van der Werff, Martijn; Warner, Harry; Spada, Fabio; Frischmuth, Thomas; Incarnato, Danny; van den Bogaart, Geert

Published in:
ChemBioChem

DOI:
10.1002/cbic.202200658

Publication date:
2023

ChemBioChem

Research Article
doi.org/10.1002/cbic.202200658

Chemistry Europe
European Chemical Societies Publishing

www.chembiochem.org

VIP *Very Important Paper*

5-Ethynyluridine: A Bio-orthogonal Uridine Variant for mRNA-Based Therapies and Vaccines

Sjors Maassen,[a] Britt Coenen,[a] Sarah-Luisa Dülk,[b] Martijn van der Werff,[a] Harry Warner,[a] Fabio Spada,[c] Thomas Frischmuth,[c] Danny Incarnato,[b] and Geert van den Bogaart*[a, d]

The identification of pseudo- and N^1-methylpseudo-uridine (Ψ and mΨ, respectively) as immunosilent uridine analogues has propelled the development of mRNA-based vaccines and therapeutics. Here, we have characterised another uridine analogue, 5-ethynyluridine (EU), which has an ethynyl moiety. We show that this uridine analogue does not cause immune activation in human macrophages, as it does not induce interleukin-6 secretion or expression of the inflammatory and antiviral genes *MX1*, *PKR*, and *TAP2*. Moreover, EU allows for prolonged expression, as shown with mRNA coding for yellow fluorescent protein (YFP). Side-by-side comparisons of EU with unmodified, Ψ, and mΨ revealed that EU-modified mRNA is expressed at lower levels, but confers similar stability and low immunogenicity to the other uridine analogues. Furthermore, structure analysis of modified mRNAs suggests that the observed phenotype is largely independent of RNA folding. Thus, EU is a potential candidate for RNA-based vaccines and therapeutics.

Introduction

The COVID-19 pandemic has accelerated the development of messenger RNA (mRNA)-based vaccines. Hundreds of millions of people worldwide have received the BNT162b2 (Pfizer/BioNTech) or mRNA-1273 (Moderna) mRNA-based vaccines, both of which induce robust adaptive immune responses against the SARS-CoV-2 virus.[1–5] The development of mRNA-based therapeutics is a revolution in vaccination strategies: Instead of direct injection of a protein antigen, host cells are transfected with lipid nanoparticle-based mRNA vaccines to transiently produce the antigen.[6] However, RNA is unstable as it is efficiently degraded by ubiquitous and interferon-inducible RNAses.[7] Moreover, RNA triggers antiviral and inflammatory immune responses due to pattern recognition receptors that bind to RNA, such as nucleotide oligomerisation domain-like receptors (NLRs), RIG–I-like receptors (RLRs) and toll-like receptors (TLRs).[8,9] The activation of these receptors initiates signalling pathways leading to the production of type I interferons (IFN), a subset of interferon-stimulated genes (ISGs), and pro-inflammatory cytokines (e.g., tumour necrosis factor alpha (TNF-α) and interleukin 6 (IL-6)),[10–15] which hamper mRNA translation through eIF2 activation by PKR (protein kinase R) and promote RNA degradation.[13,14]

To overcome this, therapeutic mRNA can be modified by replacing nucleotides with analogues that make it more resistant to degradation and less immunogenic. For example, the BNT162b2 and mRNA-1273 vaccines have all uridines replaced by N^1-methylpseudouridine (mΨ, Figure 1A). mΨ and pseudo-uridine (Ψ) supress immune sensing and enhance protein production.[16–18] Both Ψ and mΨ are naturally occurring analogues of uridine present in various types of RNA in eukaryotic cells. As a C–C rather than a N–C bond links the base and the sugar moieties in both mΨ and Ψ, the folding of mRNAs can be expected to be affected with these uridine analogues.

In this study, we investigated the stability, immunogenicity and folding of mRNA containing another uridine analogue: 5-ethynyluridine (EU). We compared this side-by-side with unmodified uridine (U), Ψ and mΨ in human peripheral blood monocyte-derived macrophages. EU has the potential added benefit of an ethynyl group, which could facilitate the selective chemical linkage of the RNA by bio-orthogonal click chemistry. Such a linkage of the RNA to chemical groups has recently been used to visualize the mRNA within transfected cells and can thereby be used to test transfection efficiency.[19] We transfected macrophages with mRNA modified with the Ψ, mΨ, and EU analogues and coding for yellow fluorescent protein (YFP) and measured YFP fluorescence levels by flow cytometry. To determine the activation of inflammatory and antiviral responses, we measured the production of IL-6 and transcription of the interferon-stimulated genes *MX1*, *PKR* and *TAP2*. Our results show that EU does not evoke immune signalling and

[a] *Dr. S. Maassen, B. Coenen, M. van der Werff, Dr. H. Warner, Prof. Dr. G. van den Bogaart*
Department of Molecular Immunology, GBB
University of Groningen
Nijenborgh 7, 9747 AG, Groningen (The Netherlands)
E-mail: G.van.den.bogaart@rug.nl
Homepage: www.mimy.eu
[b] *S.-L. Dülk, Dr. D. Incarnato*
Department of Molecular Genetics, GBB
University of Groningen
Nijenborgh 7, 9747 AG, Groningen (The Netherlands)
[c] *Dr. F. Spada, Dr. T. Frischmuth*
Baseclick GmbH
Floriansbogen 2, 82061 Neuried (Germany)
[d] *Prof. Dr. G. van den Bogaart*
Department of Medical Biology and Pathology, UMCG
Nijenborgh 7, 9747 AG, Groningen (The Netherlands)

Supporting information for this article is available on the WWW under https://doi.org/10.1002/cbic.202200658

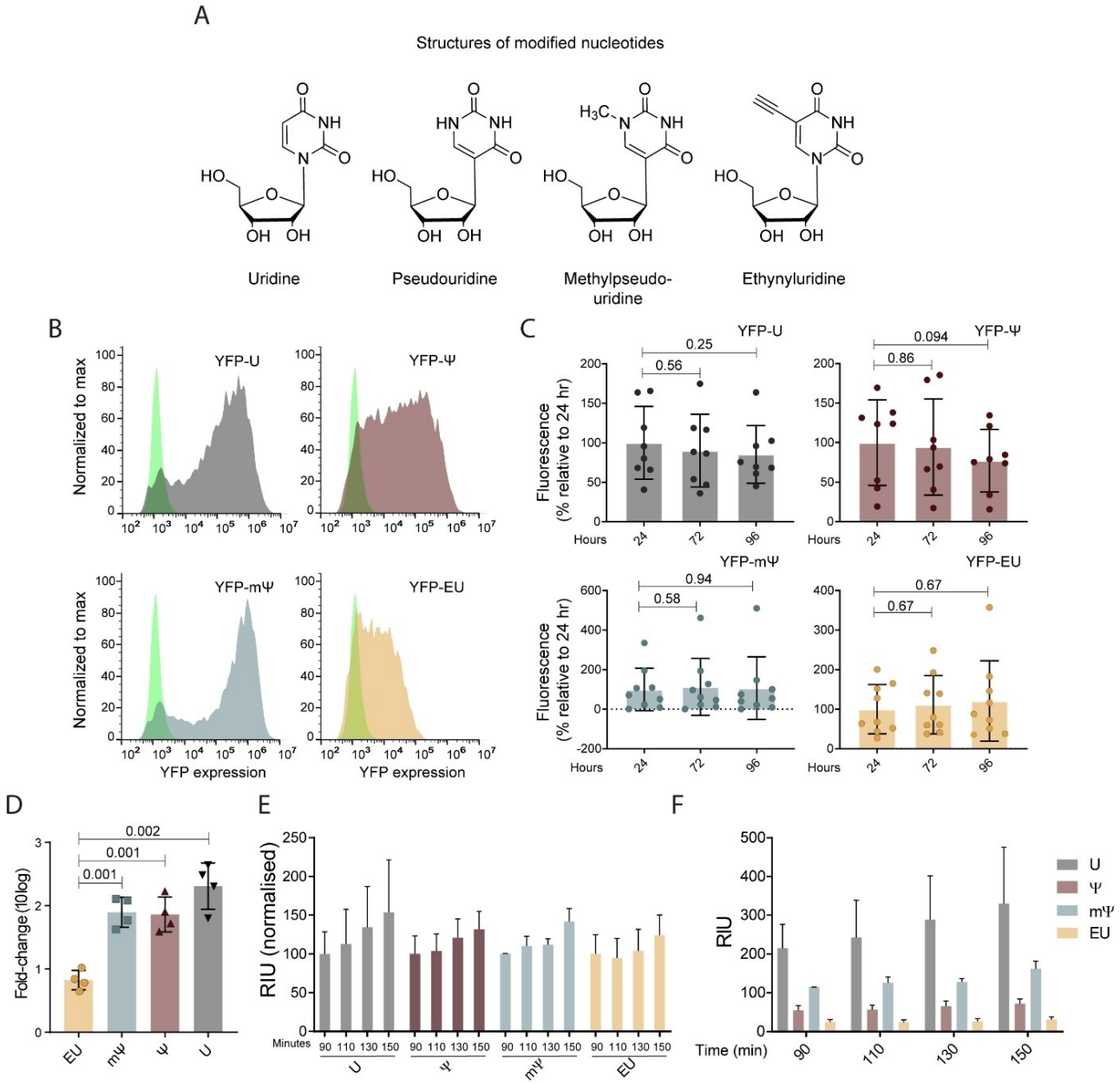

Figure 1. Effects of modified uridines in mRNA on the stability of YFP expression. A) Structures of uridine (U) and the modified nucleotides pseudouridine (Ψ), methylpseudouridine (mΨ) and ethynyluridine (EU). B) Representative flow cytometry histograms of YFP signals from macrophages transfected with mRNA containing the indicated uridine analogues and coding for YFP. The YFP signal of mock transfected cells is shown in green. C) Expression levels of YFP, expressed as percentage mean fluorescence intensity relative to average 24 h post-transfection with different mRNA constructs analysed by using flow cytometry. ($n = 10$ donors. One-way ANOVA with ANOVA with a Dunnette's multiple comparison test; *P* values shown). Mean values ± SEM. D) YFP mRNA levels detected by qPCR in mRNA transfected macrophages 48 h post-transfection ($n = 4$ donors, ANOVA followed by Dunnett's multiple comparison test). The fold change ($2^{-\Delta\Delta Ct}$) is expressed relative to pulse control. E) YFP fluorescence normalised to the 90-min time point and F) raw relative fluorescence indicated units (RIU) as measured with an in vitro translation kit ($n = 3$).

enables stable protein production, comparable to mΨ. However, the transfection efficiency of EU is lower, at least with the used electroporation protocol. Moreover, in vitro experiments showed that EU-modified mRNA is translated at lower levels than with the other uridine modifications. Finally, compared to Ψ and mΨ, the folding of EU-modified mRNA is more similar to unmodified uridine, which might be beneficial for novel RNA-based therapeutics relying on RNA folding, such as internal ribosome entry sites (IRES), ribozymes and aptamers.

Results

To compare the translation of the mRNA with the uridine analogues, human $CD14^+$ blood-derived monocytes were

differentiated to macrophages and transfected with mRNA coding for YFP. We used electroporation, as in our hands this gives far better transfection efficiencies of human monocyte-derived macrophages than lipofection agents. Monocyte-derived macrophages are terminally differentiated cells that do not divide. All uridines in the mRNA were synthesised with either EU, Ψ or mΨ, which did not influence the mRNA synthesis yields during in vitro transcription (Figure S1A in the Supporting Information). Moreover, all four variants carried identical, template-encoded 5′- and 3′-untranslated regions (UTRs) and 120-nucleotide poly(A) tail.[20] All four variants used in any given experiment were generated in parallel with the same 5′-cap structure, anti-reverse cap analogue (ARCA, a cap-0 structure[21]). The transcripts were tested for integrity and formation of secondary structures by agarose gel electrophoresis (Figure S1B). The cells were collected and measured for YFP expression by flow cytometry (Figure 1B, C; gating: Figure S1C). EU-modified mRNA has considerably lower YFP expression, as derived from the fluorescence intensity signals, than the other mRNA forms, in the order of mΨ > U > Ψ > EU for all measured timepoints. The expression levels of EU-modified mRNA were stable over time, and for most donors even went (non-significantly) up. The longest time point assessed was 96 h post-transfection, as longer time points resulted in substantial cell death for all RNA forms.

To determine whether the YFP expression levels with EU-modified RNA were caused by a lower transfection efficiency, we performed a qPCR for YFP mRNA after transfection (Figure 1D). This showed that the EU-modified mRNA levels were approximately ten-fold lower than for the other uridine analogues, and this might at least partly account for the lower YPF expression.

We also investigated the translation efficiency by conducting *in vitro* translation experiments with the YFP fluorescence as readout (Figure 1E, F; Figure S1D). All modified RNAs were translated and the YFP signal gradually increased over time (Figure 1E). However, compared to unmodified RNA, the mΨ-, EU- and Ψ-modified RNAs were two to ten times less efficiently translated, with EU-modified RNA showing the lowest (ca. 10 times lower) YFP translation (Figure 1F). As we observed this both in macrophages and in the cell-free translation assay, we conclude that differences in translation efficiency are also responsible for the variation in YFP production. However, because differences in efficiency between the modified and unmodified mRNAs are much larger with the in vitro translation kit than we observed in macrophages, the lower transfection and translation efficiencies of the modified mRNAs might be partly offset by other factors, including differential sensitivity to nucleases.

To examine the effect of the mRNA modifications on the innate immune response of the macrophages, we measured IL-6 production 24 hours post-transfection by ELISA (Figure 2A). We selected IL-6 because it is produced at high levels by activated macrophages. As a positive control, we transfected cells with the dsRNA mimetic molecule poly(I:C), which induces inflammatory and antiviral signalling via the PKR pathway through recognition by TLR3 and other pattern recognition

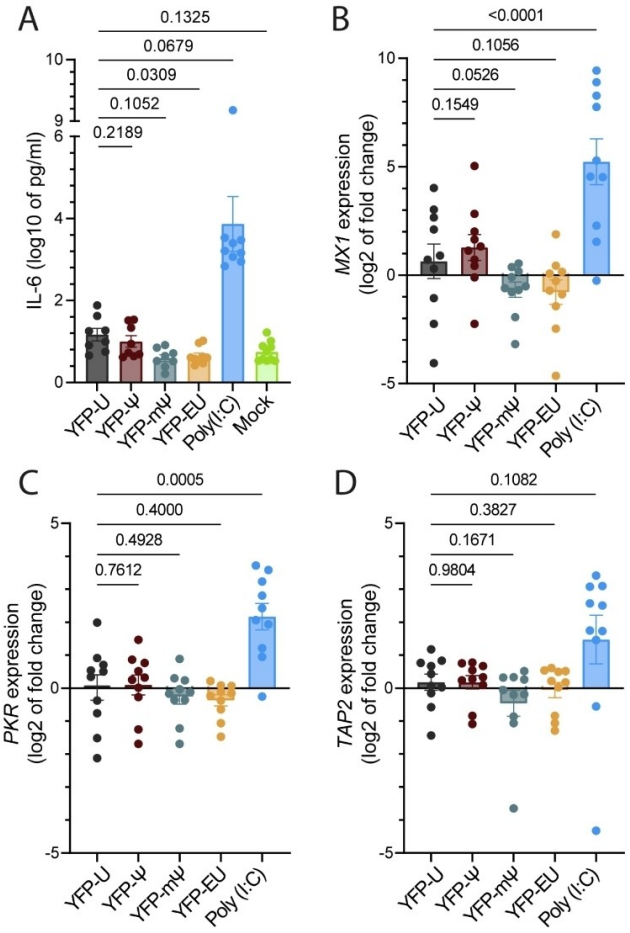

Figure 2. Effects of modified uridines on innate immune response. A) IL-6 levels in supernatant as measured by ELISA from macrophages transfected with modified YFP-coding mRNAs at 24 h post-transfection ($n = 10$ donors, unpaired t-test followed by Dunnett's multiple comparison test: *P* values shown). Transcription levels of B) *MX1*, C) *PKR* and D) *TAP2* in macrophages transfected with modified YFP-coding mRNAs at 48 h post-transfection ($n = 10$ donors, ANOVA followed by Dunnett's multiple comparison test). Gene expression ($2^{-\Delta\Delta Ct}$) is relative to control cells that were mock transfected without mRNA.

receptors such as MDA5 and PKR.[22–24] We show IL-6 levels on a logarithmic scale, as the interindividual variation in cytokine production differs over two orders of magnitude among individuals.[25,26]

IL-6 levels were low for all modified mRNAs, and was not statistically different from unmodified mRNA except for EU-modified mRNA; likely because of the large interindividual variation (Figure 2A). The production of IL-6 in the supernatant of macrophages transfected with EU-modified mRNA was significantly decreased compared to unmodified uridine. The IL-6 production by macrophages transfected with Ψ and mΨ-modified mRNA also showed a negative trend compared to unmodified mRNA, but this was not significant ($n = 10$ donors). Thus, EU-modified mRNA does not potentiate IL-6 production.

To further characterise the innate immune responses, we performed qPCR analysis for *MX1*, *PKR* and *TAP2* on macrophages transfected with mRNA containing the different uridine

modifications (Figure 2B–D). *MX1* is a downstream target of IFN type I signalling and codes for a guanosine triphosphate (GTP)-metabolising protein that impairs the replication of RNA viruses.[27] In contrast to *MX1*, *PKR* is expressed constitutively at low levels and codes for a cytosolic dsRNA sensor. After activation, *PKR* is upregulated, allowing it to block translation of most cellular and viral mRNAs and promote NF-κB activation. Finally, *TAP2*, coding for the antigen transporter involved in antigen presentation, is a downstream target of NF-κB. Although we observed no significant differences between the mRNA forms, likely again due to high interindividual variation, the expression levels of *MX1* were the highest with unmodified and Ψ-modified mRNA, with an average increase of three- to fourfold following transfection (Figure 2B). However, mΨ- and EU-modified mRNA did not affect *MX1* expression compared to the mock-transfection control. As for *PKR* and *TAP2*, their expression seemed modestly increased by unmodified and Ψ-modified mRNA, while expression was not affected or even somewhat reduced by mΨ and EU-modified mRNA (Figure 2C, D). Thus, these results support our conclusion that EU-modified mRNA, similarly to mΨ, does not induce an innate immune response in macrophages.

Next, we determined the impact of the modified uridines on the secondary structure of the mRNAs. We used selective 2′-hydroxy acylation analysed by primer extension and mutational profiling (SHAPE-MaP) with the recently developed SHAPE reagent 2-aminopyridine-3-carboxylic acid imidazolide (2 A3;[28] Figure S2). SHAPE measures the local flexibility of the RNA backbone. Highly flexible RNA residues will tend to have high SHAPE reactivity values, whereas structurally constrained residues will tend to have low SHAPE reactivity values. Pairwise correlation analysis of SHAPE reactivity profiles revealed the higher structure similarity between Ψ and mΨ-modified mRNAs (Pearson correlation coefficient $R = 0.86$), and between unmodified and EU-modified mRNAs ($R = 0.76$), although to a lower extent (Figure 3A). In-depth analysis of the distribution of SHAPE reactivities for U bases as compared to A/C/G bases (Figure 3B) revealed that Ψ and mΨ are more structurally rigid than U and EU bases, as well as than A/C/G bases. This is in line with previous analyses[29] suggesting that Ψ might work as a universal base-pairing partner, hence increasing the structural stability of duplexes. EU bases are also more structurally rigid than unmodified U bases, but to a lesser extent than Ψ and mΨ. Particularly for the EU-modified mRNA, the distribution of reactivity values for U bases and A/C/G bases shows no significant difference. Given the fact that mΨ and EU have a similar effect on the innate immune response, despite their low degree of structure similarity, while mΨ and Ψ have different effects on the innate immune response, despite their high degree of structural similarity, we can conclude that the observed phenotypes are largely independent from the folding of the mRNA.

Discussion

Ψ and mΨ are well-known immune-silent uridine analogues[30,31] that can enhance protein expression[16,30] when incorporated into mRNA. Our results are in line with the low immunogenicity of mΨ-modified mRNA and show a similarly low immune response for EU-modified mRNA. The low immunogenicity of Ψ- and mΨ-modified mRNA has been attributed to altered folding and formation of dsRNA regions, because the incorporation of Ψ changes the helical RNA conformation[29,32–34] and the incorporation of mΨ stabilizes secondary structures.[35] However, the modifications might not only reduce the detection of RNA by dsRNA sensors but might also directly mask interactions with pattern recognition receptors. Evidence for this comes from the finding that, in mice, mΨ-modified mRNA is less inflammatory even in the absence of mitochondrial antiviral signalling (MAVS), a signalling protein downstream of RLRs.[36] Moreover, experiments with exogenous

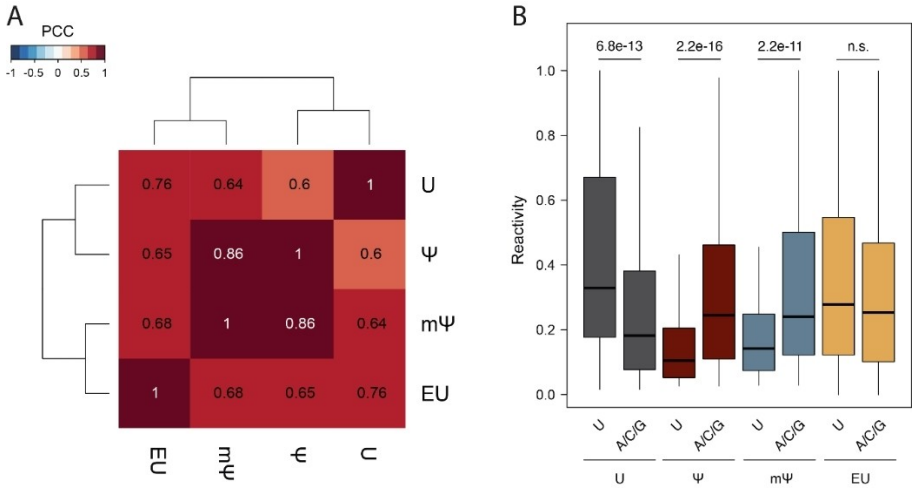

Figure 3. Modified uridines affect mRNA folding. A) Heatmap of pairwise Pearson's correlation coefficients (PCC) of SHAPE-derived reactivity profiles for in vitro synthesized transcripts or YFP-coding mRNA modified with the uridine analogues. B) Box-plots depicting the distribution of SHAPE reactivities for U bases as compared to A/C/G bases. *P* values are given by two-sided Wilcoxon Rank-Sum test.

expression of TLR7 and TLR8 in a cell line showed that the main immunosuppressive effect of mΨ is mediated through reduced activation of these TLRs.[37] This is supported by structural modelling of mΨ-modified RNA showing steric incompatibility with TLR7 binding.[34] Our findings that EU-modified mRNA has low immunogenicity while not affecting mRNA folding as much as the Ψ and mΨ modifications suggests that the EU modification also directly prevents interactions with pattern recognition receptors.

However, the low immunogenicity might come with a price, as our data indicate that EU might also affect transfection and translation by the ribosomes,[38] as EU-modified mRNA was generally expressed at lower levels than other uridine modifications, both in the macrophages and in an in vitro translation kit. Although these lower expression levels might be a disadvantage for some mRNA-based applications, they might be an advantage for other applications that rely on the prolonged expression of lower (i.e., more physiological) levels of protein. Moreover, by combining the EU and mΨ uridine analogues in a single RNA, the expression levels might be optimized for specific applications. Such a combination might provide both high and stable expression, but with the added option of bioorthogonal chemistry. For example, in the future, EU-modified mRNA might be conjugated to azide-functionalized antibodies for selective targeting to specific cell types.

Experimental Section

Macrophages: $CD14^+$ peripheral blood mononuclear cells (PMBCs) were isolated from buffy coats of donors obtained from Sanquin Bloodbank (Nijmegen, The Netherlands). Gradient centrifugation was performed at 1250*g* for 20 min at RT in SepMate-50 tubes containing ficoll. PMBCs were aspirated from the supernatant for multiple washing steps with cold PBS (4 °C) containing 1 mM EDTA and 10% BSA. The PMBCs were resuspended with Miltenyi Biotech CD14 MicroBeads (cat#: 130-050-201) for LS column (Miltenyi Biotech) magnetic antibody cell sorting (MACS) according to the manufacturer's supplied protocol. Monocytes were stored long-term in a liquid nitrogen vapour system. For differentiation, $CD14^+$ monocytes were cultured in an ultra-low-adherence 6-well plate containing complete RPMI 1640 medium (Gibco; 10% FBS, 1% L-glutamine and 1% antibiotics/antimycotics (AA), (Gibco)) supplemented with 100 ng/mL hM-CSF for 7 days. On day 3, 1 mL of complete RPMI 1640 medium containing 50 ng/mL hM-CSF was added to each well. On day 7, cells were collected from the plate with cold PBS (4 °C), centrifuged at 300×*g* for 5 min at RT, and resuspended in 5 mL PBS. Cells were counted and resuspended in 9 μL R buffer per 6×10^5 cells for transfection.

Approval to conduct experiments with human blood samples was obtained from the Dutch blood bank Sanquin and an access use agreement has been signed (NVT0459). All experiments were conducted according to national and institutional guidelines. Informed consent was obtained from all blood donors by the blood bank. Samples were anonymized and none of the investigators could ascertain the identity of the blood donors.

In vitro translation: 250 ng of mRNA was translated using the Retic lysate IVT Kit (ThermoFisher, AM1200) in a reaction volume of 50 μL. Samples were incubated at 30 °C in 96-well plates (CELLSTAR μCLEAR, black flat bottom, cat. 655090) and fluorescence intensity (λ_{ex} = 500/20 nm; λ_{em} = 541/20 nm) was measured by excitation with a 488 laser and a Cytation5 automated imager (Biotek) in 96-well plates (CELLSTAR μCLEAR, black flat bottom, cat. 655090) with 20 min intervals. The capped Xef-1 control mRNA supplied with the kit was translated in parallel to YFP mRNAs and the values from this were used to set the fluorescence background.

mRNAs: mRNAs with different modifications were obtained from baseclick GmbH (Munich, DE). Plasmids were based on pST1-2β globin UTR-A120 as described previously[20] and propagated *Escherichia coli* cells by using kanamycin for selection and isolated using the ZymoPURE Midiprep Kit (Zymo Research, cat# D4200). Plasmids were linearized by incubation with BspQI for 2 h at 50 °C and purified by using QIAquick PCR purification kit (Qiagen, cat# 28104). In vitro transcription was performed for 2 h at 37 °C, with T7 RNA polymerase (ThermoFisher Scientific; 0.6 U/μL) in a mix containing the corresponding Transcription buffer (1x), linearized plasmid (20 ng/μL), anti-reverse cap analogue (ARCA, 6.4 mM, Jena Bioscience), GTP (1.6 mM), 2.0 mM each of ATP, CTP and UTP/ΨUTP/N1-mΨUTP/EUTP as well as RNase inhibitor (ThermoFisher Scientific or Jena Biosciences; 1 U/μL). Each set of transcription reactions included samples with unmodified and all individual modified nucleotides. RNA was purified using RNA Clean & Concentrator-25 kit (Zymo Research, cat# R1017), RNA concentration was measured by fluorometry (Quibit RNA BR assay), and integrity was assessed by agarose gel electrophoresis in standard 0.5x TAE buffer and in the presence (denaturing gels) or absence (native gels) of 50 mM guanidinium isothiocyanate (Figure S1B).[39]

Transfection: Transfection was performed using the Neon Transfection System (Invitrogen), with 1 μg of mRNA per 6×10^5 cells used for electroporation (2 pulses of 40 ms, 1000 V). After transfection, the cells were divided over three 96-well round-bottom low-adherence plates and one 24-well plate for further experimentation. Cells were kept in antibiotic-free and serum-free RPMI medium (Gibco) for 3 h before the addition of 20% FBS. After 24, 72 and 96 hours post-transfection, the 96-well plates were centrifuged at 300 rpm for 5 min at RT, after which 50 μL of supernatant was collected and frozen at −20 °C. The cells were transferred to a 96-well V-bottom plate and washed once with 100 μL RPMI medium, after which the cells were resuspended in 100 μL RPMI medium for flow cytometry analysis on the CytoFLEX S (Beckman Coulter).

ELISA: IL-6 ELISA of the supernatant at 24 h post-transfection was conducted in Greiner Bio-one flat-bottom 96-well plates (Ref#: 655092) using the IL-6 Human Elisa Kit (Invitrogen, cat#: KHC0061).

RNA isolation, cDNA synthesis and qPCR: At 48 h post-transfection, total RNA from 3×10^5 transfected macrophages per condition were isolated using Quick-RNA Miniprep Kit (Zymo Research, cat# R1055) according to the manufacturers supplied protocol. For the generation of cDNA, a master mix I (1 μL random primers (100 μM, Roche), 2 ng/well total RNA, 1 μL dNTPs (10 mM, Invitrogen) and H_2O) was made. This mix was incubated at 65 °C for 5 min and directly chilled on ice for 3 min. Master mix II (4 μL of First Strand Buffer (5x, Invitrogen), 2 μL DTT (0.1 M, Invitrogen)) was added, and the samples were incubated at 37 °C for 3 min. 1 μL of M–MLV Reverse Transcriptase (Invitrogen) was added, and the samples were incubated at RT for 10 min, 37 °C for 50 min and 70 °C for 15 min, respectively. After cDNA synthesis, qPCR was performed using 5 μL PowerUp SYBR Green Master Mix (Thermo Fisher), 2 μL primer mix (10 μM), cDNA (2 ng) and H_2O tot a total of 10 μL per well and analysed on a Bio-Rad CFX96 Real-Time System. The qPCR program consisted of the following steps: 50 °C for 2 minutes, 95 °C for 2 min, 95 °C for 15 s, 60 °C for 1 min, of which the latter two were repeated 40 times. The following primers were used for qPCR: *MX1*, forward: GGCTGTTTACCAGACTCCGACA, reverse: CACAAAGCCTGGCAGCTCTCTA; *PKR*, forward: GAAGTGGACCTCTACGCTTT-

GG, reverse: TGATGCCATCCCGTAGGTCTGT; *TAP2*, forward: ATGCCCTTCACAATAGCAGCGG, reverse: CCAAAACTGCGAACGGTCTGCA; *SNRPD3*, forward: GGAAGCTCATTGAAGCAGAGGAC, reverse: CAGAAAGCGGATTTTGCTGCCAC and YFP, forward: GCACGACTTCTTCAAGTCCGCCATGCC, reverse: GCGGATCTTGAAGTTCACCTTGATGCC. All PCRs were normalised to reference gene *SNRPD3*,[40,41] and relative expression levels were determined by the $\Delta\Delta C_t$ method.

In vitro probing and folding: RNA in a volume of 39 μL was denatured at 95 °C for 2 min, then transferred to ice for 1 min. 10 μL of ice-cold 5x RNA Folding Buffer (500 mM HEPES pH 7.9; 500 mM NaCl) supplemented with 20 U of SUPERase·In RNase Inhibitor (ThermoFisher) were added. RNA was then incubated for 15 min at 37 °C to allow secondary structure formation. Subsequently, 1 μL of 500 mM $MgCl_2$ (pre-warmed at 37 °C) was added, and RNA was further incubated for 15 min at 37 °C to allow tertiary structure formation. For probing of RNA, 2-aminopyridine-3-carboxylic acid (2 A3[28]) was added to a final concentration of 100 mM (assuming a stock concentration of 1 M). An equal volume of DMSO was added to the control samples. Samples were then incubated at 37 °C for 5 min. Reactions were quenched by adding 1 volume DTT 1 M and then purified on Monarch RNA Cleanup Kit columns (NEB).

SHAPE-MaP library preparation: Both DMSO- and 2 A3-treated samples were fragmented in a buffer containing 4 mM final $MgCl_2$ by incubating at 94 °C for 8 min. Fragmented RNA was purified on Monarch RNA Cleanup Kit columns. Fragmented RNA was end-repaired by treatment with 1 U of rSAP (NEB) at 37 °C for 30 min, plus 5 min at 70 °C to heat-inactivate the enzyme, followed by treatment with 20 U of T4 PNK (NEB) in the presence of 1 mM ATP at 37 °C for 1 h. The end-repaired RNA was then used as input for the NEBNext Small RNA Library Prep Set for Illumina until just before the reverse-transcription step. At this point, the adapter-ligated RNA was re-purified on Monarch RNA Cleanup Kit columns and subjected to reverse transcription, as per standard SHAPE-MaP conditions. Briefly, RNA in 9 μL NF H_2O was mixed with 1 μl of 10 mM SR RT Primer (AGACGTGTGCTCTTCCGATCT) and 1 μL 10 mM dNTPs, then incubated at 70 °C for 5 min, and immediately transferred to ice for 1 min. Then, 4 μL of 5x RT Buffer (250 mM Tris pH 8.0; 375 mM KCl), 2 μl of DTT (0.1 M), 1 μL of SuperaseIN RNase inhibitor (Ambion), 1 μL of SuperScript II RT (ThermoFisher Scientific), and 1 μL 120 mM MnCl2 were added, the reactions mixed, and incubated at 42 °C for 2 hours. Reactions were cleaned up on Monarch RNA Cleanup Kit columns, following the protocol for purifying RNA fragments larger than 200 nucleotides. Barcodes were then introduced by PCR, using NEBNext High-Fidelity 2X PCR Master Mix (NEB) and NEBNext Multiplex Oligos for Illumina Dual-Index primers (NEB).

SHAPE-MaP data analysis: All the analysis steps, from reads alignment to data normalisation, were performed using RNA Framework,[42] available from: https://github.com/dincarnato/RNA-Framework.

Statistical analysis: Statistical analysis was done using GraphPad software. One-way ANOVA was applied for comparisons followed by a post hoc Dunnett's test. For SHAPE-MaP, a two-sided Wilcoxon Rank-Sum test was performed. All data are presented as mean ± SEM, and significance was assumed when $p < 0.05$.

Author Contributions

S.M. and B.C. did all the macrophage experiments, graph making and the writing together with G.v.d.B. F.S. and T.F. made all mRNAs and provided manuscript feedback. D.I. and S.D. analysed the structure of the mRNA and provided input into the manuscript. M.v.d.W. conducted analysis.

In this publication we tested the applicability of the synthetic uridine analogue 5-ethynyl uridine (EU) for use in RNA-based therapies and vaccines. The patented uridine analogue N^1-methylpseudouridine is mostly used In current RNA-based vaccines, due to its lower immunogenicity and stronger expression compared to unmodified uridine. In this study, we investigated the immunogenicity and expression of EU. EU has the added benefit of a click-chemistry handle for functionalisation of RNA (e.g., conjugation to a chemical moiety for drug targeting or enhancing endosomal escape). EU was compared side-by side with unmodified, pseudo- and N^1-methylpseudouridine in human blood monocyte-derived macrophages using electroporation with modified mRNAs coding for YFP. By measuring interferon-stimulated genes (ISGs), we demonstrate the extend by which autocrine signalling due to interferon type I secretion is induced by these uridine-analogous that signal back into the cell by interferon-α/β receptor (IFNAR). Most notable from this investigation is that N^1-methylpseudouridine and EU showed comparable immunogenicity and stable expression. However, EU showed lower YFP expression levels, both in transfected cells and with an in vitro translation kit. Finally, compared to the other modifications, EU-modified RNA folded more similarly to unmodified RNA. Novel uridine analogues could be an asset to the development of RNA-based drugs.

Acknowledgements

This work was supported by the European Research Council (ERC) under the European Union's Horizon 2020 research innovation programme [grant agreement no. 862137] to G.v.d.B.; ZonMW [project grant no. 09120011910001] to G.v.d.B. The authors would like to acknowledge Pieter Grijpstra for his very competent management of lab utilities during the COVID-19 pandemic to assure completion of this project.

Conflict of Interest

F.S. and T.F. are employees of baseclick GmbH, which has developed a platform for chemo-enzymatic modification of in vitro transcribed RNA, including development of an own mRNA-based vaccine, and provides custom mRNA services.

Data Availability Statement

The data that support the findings of this study are available on Zenodo under the entry 7298648.

Keywords: macrophage · mRNA therapy · uridine analogues · viral immunity

[1] M. J. Mulligan, K. E. Lyke, N. Kitchin, J. Absalon, A. Gurtman, S. Lockhart, K. Neuzil, V. Raabe, R. Bailey, K. A. Swanson, P. Li, K. Koury, W. Kalina, D. Cooper, C. Fontes-Garfias, P. Y. Shi, Ö. Türeci, K. R. Tompkins, E. E. Walsh, R. Frenck, A. R. Falsey, P. R. Dormitzer, W. C. Gruber, U. Şahin, K. U. Jansen, *Nature* **2020**, *586*, 589–593.
[2] N. Dagan, N. Barda, E. Kepten, O. Miron, S. Perchik, M. A. Katz, M. A. Hernán, M. Lipsitch, B. Reis, R. D. Balicer, *N. Engl. J. Med.* **2021**, *384*, 1412–1423.
[3] F. P. Polack, S. J. Thomas, N. Kitchin, J. Absalon, A. Gurtman, S. Lockhart, J. L. Perez, G. Pérez Marc, E. D. Moreira, C. Zerbini, R. Bailey, K. A. Swanson, S. Roychoudhury, K. Koury, P. Li, W. V. Kalina, D. Cooper, R. W. Frenck, L. L. Hammitt, Ö. Türeci, H. Nell, A. Schaefer, S. Ünal, D. B. Tresnan, S. Mather, P. R. Dormitzer, U. Şahin, K. U. Jansen, W. C. Gruber, *N. Engl. J. Med.* **2020**, *383*, 2603–2615.
[4] L. A. Jackson, E. J. Anderson, N. G. Rouphael, P. C. Roberts, M. Makhene, R. N. Coler, M. P. McCullough, J. D. Chappell, M. R. Denison, L. J. Stevens, A. J. Pruijssers, A. McDermott, B. Flach, N. A. Doria-Rose, K. S. Corbett, K. M. Morabito, S. O'Dell, S. D. Schmidt, P. A. Swanson, M. Padilla, J. R. Mascola, K. M. Neuzil, H. Bennett, W. Sun, E. Peters, M. Makowski, J. Albert, K. Cross, W. Buchanan, R. Pikaart-Tautges, J. E. Ledgerwood, B. S. Graham, J. H. Beigel, *N. Engl. J. Med.* **2020**, *383*, 1920–1931.
[5] U. Sahin, A. Muik, E. Derhovanessian, I. Vogler, L. M. Kranz, M. Vormehr, A. Baum, K. Pascal, J. Quandt, D. Maurus, S. Brachtendorf, V. Lörks, J. Sikorski, R. Hilker, D. Becker, A. K. Eller, J. Grützner, C. Boesler, C. Rosenbaum, M. C. Kühnle, U. Luxemburger, A. Kemmer-Brück, D. Langer, M. Bexon, S. Bolte, K. Karikó, T. Palanche, B. Fischer, A. Schultz, P. Y. Shi, C. Fontes-Garfias, J. L. Perez, K. A. Swanson, J. Loschko, I. L. Scully, M. Cutler, W. Kalina, C. A. Kyratsous, D. Cooper, P. R. Dormitzer, K. U. Jansen, Ö. Türeci, *Nature* **2020**, *586*, 594–599.
[6] J. A. Wolff, R. W. Malone, P. Williams, W. Chong, G. Acsadi, A. Jani, P. L. Felgner, *Science* **1990**, *247*, 1465–1468.
[7] A. Sadler, B. Williams, *Nat. Rev. Immunol.* **2008**, *8*, 559–568.
[8] T. Kawai, S. Akira, *Nat. Immunol.* **2006**, *7*, 131–137.
[9] J. Sprent, C. King, *Sci. Immunol.* **2021**, *6*, 10.1126/SCIIMMUNOL.ABJ9256.
[10] O. V Sergeeva, V. E. Koteliansky, T. S. Zatsepin, *Biochemistry* **2016**, *81*, 709–722.
[11] A. De Beuckelaer, J. Grooten, S. De Koker, *Trends Mol. Med.* **2017**, *23*, 216–226.
[12] Z. Zhong, S. Mc Cafferty, F. Combes, H. Huysmans, J. De Temmerman, A. Gitsels, D. Vanrompay, J. Portela Catani, N. N. Sanders, *Nano Today* **2018**, *23*, 16–39.
[13] S. Linares-Fernández, C. Lacroix, J. Y. Exposito, B. Verrier, *Trends Mol. Med.* **2020**, *26*, 311–323.
[14] J. Devoldere, H. Dewitte, S. C. De Smedt, K. Remaut, *Drug Discovery Today* **2016**, *21*, 11–25.
[15] W. M. Schneider, M. D. Chevillotte, C. M. Rice, *Annu. Rev. Immunol.* **2014**, *32*, 513–545.
[16] K. Karikó, H. Muramatsu, J. Ludwig, D. Weissman, *Nucleic Acids Res.* **2011**, *39*, 10.1093/nar/gkr695.
[17] O. Andries, S. Mc Cafferty, S. C. De Smedt, R. Weiss, N. N. Sanders, T. Kitada, *J. Controlled Release* **2015**, *217*, 337–344.
[18] K. Karikó, H. Muramatsu, F. A. Welsh, J. Ludwig, H. Kato, S. Akira, D. Weissman, *Mol. Ther.* **2008**, *16*, 1833–1840.
[19] S. Croce, S. Serdjukow, T. Carell, T. Frischmuth, *ChemBioChem* **2020**, *21*, 1641–1646.
[20] S. Holtkamp, S. Kreiter, A. Selmi, P. Simon, M. Koslowski, C. Huber, Ö. Türeci, U. Sahin, *Blood* **2006**, *108*, 4009–4017.
[21] J. Stepinski, C. Waddell, R. Stolarski, E. Darzynkiewicz, R. E. Rhoads, *RNA* **2001**, *7(10)*, 1486–1495.
[22] X. Mu, E. Greenwald, S. Ahmad, S. Hur, *Nucleic Acids Res.* **2018**, *46*, 5239–5249.
[23] S. Vaidyanathan, K. T. Azizian, A. K. M. A. Haque, J. M. Henderson, A. Hendel, S. Shore, J. S. Antony, R. I. Hogrefe, M. S. D. Kormann, M. H. Porteus, A. P. McCaffrey, *Mol. Ther. Nucleic Acids* **2018**, *12*, 530–542.
[24] K. Karikó, H. Ni, J. Capodici, M. Lamphier, D. Weissman, *J. Biol. Chem.* **2004**, *279*, 12542–12550.
[25] R. ter Horst, M. Jaeger, S. P. Smeekens, M. Oosting, M. A. Swertz, Y. Li, V. Kumar, D. A. Diavatopoulos, A. F. M. Jansen, H. Lemmers, H. Toenhake-Dijkstra, A. E. van Herwaarden, M. Janssen, R. G. van der Molen, I. Joosten, F. C. G. J. Sweep, J. W. Smit, R. T. Netea-Maier, M. M. J. F. Koenders, R. J. Xavier, J. W. M. van der Meer, C. A. Dinarello, N. Pavelka, C. Wijmenga, R. A. Notebaart, L. A. B. Joosten, M. G. Netea, *Cell* **2016**, *167*, 1111–1124.e13.
[26] Y. Li, M. Oosting, P. Deelen, I. Ricaño-Ponce, S. Smeekens, M. Jaeger, V. Matzaraki, M. A. Swertz, R. J. Xavier, L. Franke, C. Wijmenga, L. A. B. Joosten, V. Kumar, M. G. Netea, *Nat. Med.* **2016**, *22*, 952–960.
[27] D. Holzinger, C. Jorns, S. Stertz, S. Boisson-Dupuis, R. Thimme, M. Weidmann, J.-L. Casanova, O. Haller, G. Kochs, *J. Virol.* **2007**, *81*, 7776–7785.
[28] T. Marinus, A. B. Fessler, C. A. Ogle, D. Incarnato, *Nucleic Acids Res.* **2021**, *49*, E34-E34.
[29] E. Kierzek, M. Malgowska, J. Lisowiec, D. H. Turner, Z. Gdaniec, R. Kierzek, *Nucleic Acids Res.* **2014**, *42*, 3492–3501.
[30] B. R. Anderson, H. Muramatsu, S. R. Nallagatla, P. C. Bevilacqua, L. H. Sansing, D. Weissman, K. Karikó, *Nucleic Acids Res.* **2010**, *38*, 5884–5892.
[31] M. Fotin-Mleczek, K. M. Duchardt, C. Lorenz, R. Pfeiffer, S. Ojkić-Zrna, J. Probst, K. J. Kallen, *J. Immunother.* **2011**, *34*, 1–15.
[32] D. R. Davis, *Nucleic Acids Res.* **1995**, *23*, 5020–5026.
[33] Y. C. Chang, J. Herath, T. H. H. Wang, C. S. Chow, *Bioorg. Med. Chem.* **2008**, *16*, 2676.
[34] K. D. Nance, J. L. Meier, *ACS Cent. Sci.* **2021**, *7*, 748–756.
[35] D. M. Mauger, B. Joseph Cabral, V. Presnyak, S. V. Su, D. W. Reid, B. Goodman, K. Link, N. Khatwani, J. Reynders, M. J. Moore, I. J. McFadyen, *Proc. Natl. Acad. Sci. USA* **2019**, *116*, 24075–24083.
[36] J. Nelson, E. W. Sorensen, S. Mintri, A. E. Rabideau, W. Zheng, G. Besin, N. Khatwani, S. V. Su, E. J. Miracco, W. J. Issa, S. Hoge, M. G. Stanton, J. L. Joyal, *Sci. Adv.* **2020**, *6*.
[37] K. Karikó, M. Buckstein, H. Ni, D. Weissman, *Immunity* **2005**, *23*, 165–175.
[38] M. A. Collart, B. Weiss, *Nucleic Acids Res.* **2020**, *48*, 1043–1055.
[39] S. K. Goda, N. P. Minton, *Nucleic Acids Res.* **1995**, *23*, 3357–3358.
[40] M. Esteva-Socias, F. Gómez-Romano, J. A. Carrillo-Ávila, A. L. Sánchez-Navarro, C. Villena, *Sci. Rep.* **2020**, *10*, 1–11.
[41] D. Scarlet, R. Ertl, C. Aurich, R. Steinborn, *PLoS One* **2015**.
[42] D. Incarnato, E. Morandi, L. M. Simon, S. Oliviero, *Nucleic Acids Res.* **2018**, *46*, 10.1093/NAR/GKY486.

Manuscript received: November 11, 2022
Revised manuscript received: December 17, 2022
Accepted manuscript online: January 3, 2023
Version of record online: January 31, 2023